Experimental Methods to Evaluate the Impact of a Photovoltaic System at the Point of Common Coupling in Low Voltage Networks

Gianfranco Chicco [(1)], Luca Giaccone [(1)], Filippo Spertino [(1)] and Giorgio Graditi [(2)]
(1) Politecnico di Torino - Dipartimento di Ingegneria Elettrica
Corso Duca degli Abruzzi 24 - 10129 Torino, Italy
Tel: +39-011-5647120; fax +39-011-5647199 - Email: filippo.spertino@polito.it
(2) Centro Ricerche ENEA - Ente per le Nuove Tecnologie, l'Energia e l'Ambiente
Via Vecchio Macello - 80055 Portici, Napoli, Italy
Tel: +39-081-7723400; fax: +39-081-7723344 - Email: giorgio.graditi@portici.enea.it

***Abstract* — After the presentation of the limits within which it is possible to define the equivalent impedance of the network, the focus of the paper, at this aim, is on two measuring methods. The first one is based on grid perturbation, due to current injection of PhotoVoltaic (PV) inverters, whereas the second one is based on grid perturbation, due to current injection of load standards (resistive or capacitive). The experimental results, related to some PV systems, show relatively high values of impedances (≈ 1 Ω) with respect to the values calculated under simplified assumptions. For all the PV systems analysed, the results show that it is possible to upgrade further the PV systems without particular problems of voltage rise on the grid.**

Keywords – **Network impedance, photovoltaic power systems, test facilities, voltage rise.**

I. INTRODUCTION

Worldwide in the growing energy markets the Distributed (or Dispersed) Generation (DG) is a possible option for consumers of electrical energy who ask for energy saving and feed-in tariffs as incentives for renewable energies or cogeneration (i.e. combined heat/power). Other goals that can be achieved with DG are peak shaving, standby power, grid support in case of remarkable voltage drops or power losses in the distribution lines.

The corresponding technologies can include gas micro-turbines, fuel cells and renewable energies as wind turbines and PhotoVoltaic (PV) generators. All these types of power sources can be equipped with DC-AC converters (inverters) at the grid interface. In this paper only the inverters supplied by PV generators are analysed, but the proposed method to evaluate the impact on the grid can be applied also to other solutions with inverter-based grid interface.

To supply the AC loads of users, the distributed grid connected PV systems are essentially composed of arrays of PV modules and inverters connected to the Low Voltage (LV) network. The inverter, with associated functions for obtaining optimum interface between the DC side and the AC side (e.g. unitary power factor), is the key-component for successful operation of the grid connected PV system. This component, with the Maximum Power Point Tracker (MPPT) and the grid interface protections, forms the so-called Power Conditioning Unit (PCU).

During the installation of a DG system, it is important *to assess the network (grid) impedance* at the Point of Common Coupling (PCC), since the *voltage rise*, when the DG system gives the rated power, can exceed the limits imposed by the network distributor [1]. Actually, the voltage rise can cause the automatic disconnection of the DG system which must be equipped with over/under voltage relays, besides the over/under frequency ones. In order to evaluate the impact of a PV system at the PCC, also in terms of *maximum PV power capacity*, it is necessary to define the parameters of the distribution network.

Different methods have been proposed and tested for measuring the grid impedance: transients-based methods and steady-state-based methods or passive and active methods. Generally, they are based on a load standard (capacitive and/or resistive), that can be switched on or off iteratively; in any case, the measurement uncertainty is not negligible [2], [3], [4], [5].

In this paper, within the steady-state methods, *another possible method* (here named the "PV inverter" method) to measure the network impedance, besides the mentioned "load standard" method, is presented: it is based on a rapid switching from load condition to no-load condition.

II. THEORETICAL REMARKS

With reference to a single-phase equivalent circuit, in which the impedances are concentrated into the phase wire without inserting impedances in the neutral one, the DG behaviour (here PV generator) is assumed as that of a current source $\underline{I}_{PV}$, depending on solar irradiance. The grid behaviour is assumed as that of a Thévenin generator, in which the voltage source $\underline{E}_{Th}$ and the equivalent impedance $\underline{Z}_{Th}$ take into account different contributions:

- the e.m.f. of LV windings of MV-LV transformer $\underline{E}_T$;
- the MV grid impedance $\underline{Z}_{MVg}$ and the short circuit impedance of MV-LV transformer $\underline{Z}_{scT}$;
- the impedances of LV lines $\underline{Z}_{LVl}$ (by neglecting the capacitive parameters if they are below a given limit);
- the corresponding impedances $\underline{Z}_L$ of the loads supplied by these lines (however, many times, it is not

1-4244-0194-1/06/$20.00 ©2006 IEEE

possible to define a constant impedance when the loads are non-linear as for power electronics, discharge lamps, electro-magnetic machines in no-load condition,…).

Fig. 1 shows an example with two lines and two loads. The value of the equivalent impedance, assumed as $\underline{Z}_{grid}$, depends on the PCC: if it is at the beginning of the lines, near the transformer, as in case (a), the voltage drop and power losses are not influenced; the situation changes if it is at the end, near the loads, as in case (b) with line # 2 which supplies $\underline{Z}_{L2}$.

Usually, as a first approximation, $\underline{Z}_{L}$ of the loads are considered infinite in the calculation of $\underline{Z}_{grid}$ and so in the case a. it results $\underline{Z}_{grid} = \underline{Z}_{MVg} + \underline{Z}_{scT}$, while in the case b. it results $\underline{Z}_{grid} = \underline{Z}_{MVg} + \underline{Z}_{scT} + \underline{Z}_{LVl2}$.

In the latter case, the value of $\underline{Z}_{grid}$ could be so high that the PV power capacity should be reduced, in order to fulfill the voltage-quality requirements.

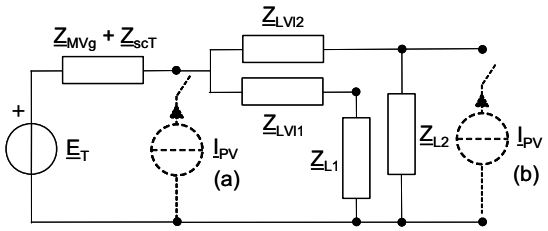

Fig. 1. PCC at the beginning or at the end of the LV lines (# 2).

III. THE PV INVERTER METHOD

The "PV inverter" method is based on two typical tests, to be carried out as close as possible, because the load conditions of the network must not be different [6]. The first test is performed with the DG system operating close to the rated power (load condition) and the other test without the DG system (no-load condition). Then, it is necessary to process the waveform data for defining the phasors by the Discrete Fourier Transform (DFT).

Now focusing the attention on the experimental tests, by means of a suitable Automatic Data Acquisition System (ADAS), it is possible to measure the waveforms (usually 5-10 periods with 500-1000 samples/period and 12-bit resolution) at the PCC in the two tests. Then, the magnitude (r.m.s. value) and the phase of voltage and current phasors can be obtained by assuming as reference the phase of the grid voltage without the PV inverter $\underline{E}_{Th}$; here it is defined as $\underline{V}_0$ because it is measured with the DG generator switched off.

In Fig. 2a) - 2b) the equivalent and the measuring circuits for grid impedance assessment, according to this method, are shown.

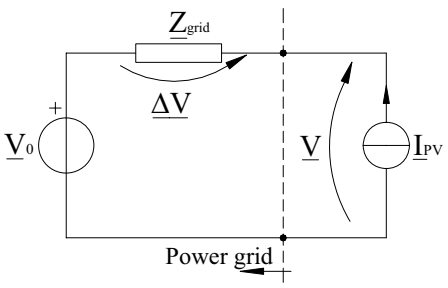

2a)

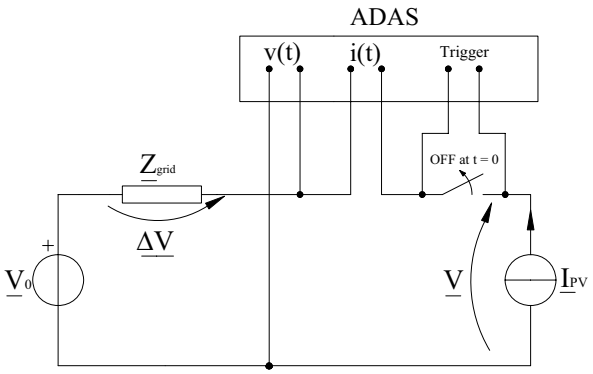

2b)

Fig. 2. Equivalent and measuring circuits in the PV inverter method.

As a first approximation, only the fundamental harmonic of the DFT of the waveforms can be considered: this is a good choice for the voltage waveforms which are slightly distorted, but it cannot be the same for the current waveform because it depends on the quality of the inverter. Actually, some inverters provide the rated current with Total Harmonic Distortion (THD) around 10%.

It is worth noting that, in the case of PV inverters, the current sinusoid should be in phase with the grid voltage sinusoid for complying with the technical regulations (e.g., European Standards [7]). In practice, depending on the loading condition, the phasors $\underline{V}$ and $\underline{I}_{PV}$ have different phase angles: in Fig. 3 the grid behaves, in terms of reactive power, as an inductor with the angle of current φ lower than the angle of voltage θ, while the voltage difference $\underline{\Delta V}$ has the greatest angle δ. This latter one means that the grid impedance has an inductive component, as usual. Finally, the phase reference corresponds to the no-load condition ($\underline{V}_0$).

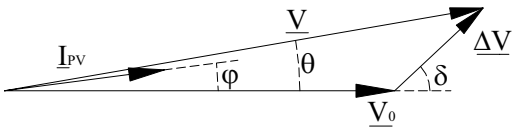

Fig. 3. Phasor diagram of $\underline{V}_0$, $\underline{V}$ and $\underline{I}_{PV}$ in the PV inverter method.

III.1. The Assessment of Grid Impedance

By considering the phasor diagram in Fig. 3, the Thévenin impedance can be calculated as in the following:

$$\overline{Z}_{grid} = \frac{\overline{V} - \overline{V}_0}{\overline{I}_{PV}} = \frac{V\cos\theta - V_0 + jV\sin\theta}{I_{PV}e^{j\varphi}} = \frac{\Delta V}{I_{PV}}e^{j(\delta-\varphi)} \quad (1)$$

In the previous expression, the calculation of the impedance, both in magnitude and in angle, is affected by high uncertainty because the differences ($V\cdot\cos\theta - V_0$) and (δ-φ) can be low: consequently, the values of resistance and reactance, besides their share, are not well determined. In particular, since *the first difference*, i.e., the voltage rise, can be 1-7V with respect to V_0 = 220-240V, the accuracy of measurement for the two terms must have more than 3 significant digits. Furthermore, the imaginary part $V\cdot\sin\theta$ of the phasor $\underline{V}$, normally very low, has high uncertainty and thus the selection of the

reference for the phase angles must be different: the new reference is chosen so as to have about π/4 rad for the $\underline{V}_0$ phasor.

By this assumption, in Fig. 4 the *common reference* for the phase of the voltage and current signals is represented with two periods of the waveforms (voltage and current) before the PV switch off, and two periods of the waveform (voltage) after the PV switch off.

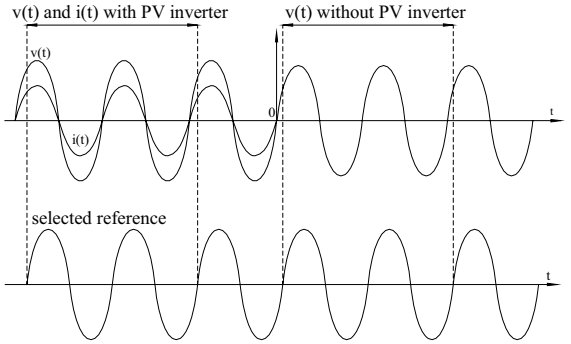

Fig. 4. The "virtual" common reference in the PV inverter method.

Therefore, if the deterministic method is used for the uncertainty calculation in an indirect measurement (as in this case), the start point for the propagation formula of uncertainty is the following:

$$\overline{Z}_{grid} = \frac{V\cos\theta - V_0\cos\theta_0 + j\left(V\sin\theta - V_0\sin\theta_0\right)}{I_{PV}e^{j\varphi}} \qquad (2)$$

As an example, the relative uncertainties for both real ($\varepsilon_{Re(\underline{V})}$) and imaginary ($\varepsilon_{Im(\underline{V})}$) parts of the phasor $\underline{V}$ are reported:

$$\varepsilon_{\mathrm{Re}(\overline{V})} = \varepsilon_V + |\Delta\theta|\cdot|\tan\theta| \quad \varepsilon_{\mathrm{Im}(\overline{V})} = \varepsilon_V + |\Delta\theta|/|\tan\theta| \qquad (3)$$

in which the typical relative uncertainty on r.m.s. value ε_V = 0.05% and the typical absolute uncertainty on phase angle $\Delta\theta \approx 0.006$ rad. Furthermore, the uncertainty grows when the difference $\underline{\Delta V}$ is calculated (25-30%), here only the relative uncertainties on the real part and on the magnitude are shown:

$$\varepsilon_{\mathrm{Re}(\Delta\overline{V})} = \frac{\left|\mathrm{Re}(\overline{V})\right|\varepsilon_{\mathrm{Re}(\overline{V})} + \left|\mathrm{Re}(\overline{V}_0)\right|\varepsilon_{\mathrm{Re}(\overline{V}_0)}}{\left|\mathrm{Re}(\overline{V}) - \mathrm{Re}(\overline{V}_0)\right|} \qquad (4)$$

$$\varepsilon_{\Delta V} = \frac{\left[\mathrm{Re}(\Delta\overline{V})\right]^2\varepsilon_{\mathrm{Re}(\Delta\overline{V})} + \left[\mathrm{Im}(\Delta\overline{V})\right]^2\varepsilon_{\mathrm{Im}(\Delta\overline{V})}}{\left[\mathrm{Re}(\Delta\overline{V})\right]^2 + \left[\mathrm{Im}(\Delta\overline{V})\right]^2} \qquad (5)$$

Then, the relative uncertainty on the magnitude of the impedance depends also on the uncertainty of the r.m.s. current value $\varepsilon_{Ipv} \approx 1\%$. Finally, it results that, for the network impedance, the relative uncertainties are $\varepsilon_{Zgrid} \approx 30\%$ on the magnitude, $\varepsilon_{\varphi Zgrid} \approx 30\%$ on the characteristic angle, $\varepsilon_{Rgrid} \approx 35\%$ on the real part and $\varepsilon_{Xgrid} \approx 40\%$ on the imaginary part.

IV. THE LOAD STANDARD METHOD

Also the "Load Standard" method is based on two typical tests, to be carried out as close as possible, because the load conditions of the network must not be different. The first test is performed without the load standard (no-load condition) and the other test under loading condition. Similarly, it is necessary to process the waveform data for defining the phasors by DFT.

By using the same ADAS, in Fig. 5a) - 5b) the equivalent and the measuring circuits for grid impedance assessment, according to this method, are shown.

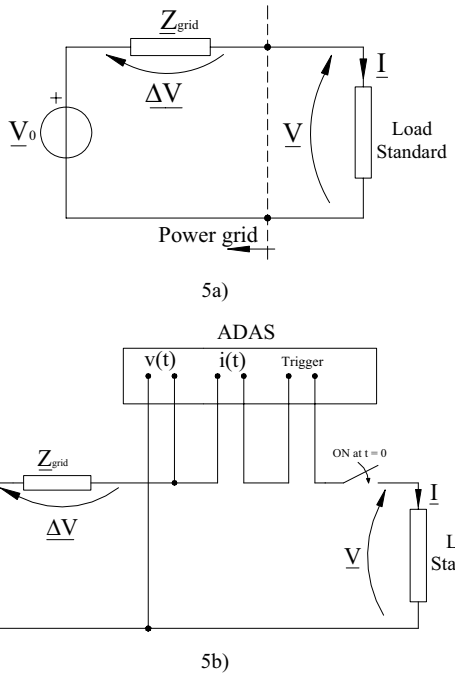

Fig. 5. Equivalent and measuring circuits in the load standard method.

As a first approximation, only the fundamental of the DFT of the waveforms can be considered: this is a good choice for the voltage waveforms which are slightly distorted (THD_V = 2-3%), but it cannot be the same for the current waveform because it depends on the type of load. If the load standard is a capacitor, THD_I can be greater than 10%, in fact it should be remembered that the harmonic currents I_{Ch} in a capacitor are:

$$I_{Ch} = h\omega C V_{Gh} \qquad (6)$$

where h is the harmonic order, $\omega \approx 314$ rad/s, C is the capacitance and V_{Gh} is the grid contribution of harmonic voltage.

Contrary to the PV inverter method, here a *voltage drop* occurs if the load standard is a resistor, while the voltage is almost constant if the load standard is a capacitor: only a *little rotation* of the phasor $\underline{V}$ (low change of phase angle) occurs. Fig. 6 shows the phasor diagram with a resistor as load standard and hence a voltage drop takes place; moreover, since the grid impedance has an inductive reactance, the no-load voltage $\underline{V}_0$ has an angle greater than the one of the resistor voltage $\underline{V}$.

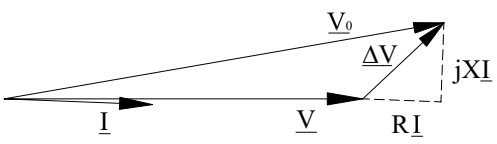

Fig. 6. Phasor diagram of $\underline{V}_0$, $\underline{V}$ and $\underline{I}$ in the load-standard method.

Now, the evaluation of the network impedance follows the previous procedure, remembering that:

$$\overline{Z}_{grid} = \frac{\overline{V}_0 - \overline{V}}{\overline{I}} \quad (7)$$

Similar issues can be drawn about the common reference and the measurement uncertainty.

V. Experimental Results

Three PV plants, connected to the 400V three-phase grid, have been analysed:

1. a 20kW$_p$ generator, property of the municipal company for waste management (AMIAT - Torino);
2. a 20kW$_p$ generator, property of the "Provincia di Cuneo" public administration;
3. a 16kW$_p$ generator, property of the public company "Environment Park - Torino";

The systems # 1 and # 2 are equipped with 6 single-phase inverters, two parallel-connected per each phase. On the other hand, the system # 3 is equipped with 8 single-phase inverters, three for phase R, three for phase S and two for phase T with respect to the neutral wire N: that is due to the PV arrays which have 8 different tilt angles.

As an example, the structure of LV grid for system # 1 includes, as main components, two equal parallel-connected MV/LV transformers with 315 kVA nominal power and 6% short-circuit voltage; a three-phase cable line of 300 m (cross-section 185 mm^2 for the phase conductors and 120 mm^2 for the neutral conductor); a final three-phase + neutral cable of 20 m and cross-section 10 mm^2.

By neglecting the system loads, as said in paragraph II, the Thévenin equivalent impedance, at the point of connection of each of the six single-phase inverters, is $Z_{grid} \approx 200m\Omega$ with characteristic angle of about 20°. Nevertheless, the Thévenin equivalent impedance could be much higher in systems with lower size of the MV/LV transformer and longer cable lines.

As an example of the PV inverter method, Fig. 7 shows the experimental results concerning the PV system # 3, in which the r.m.s. *voltage rise* is around 7V with a r.m.s. value I_{PV} = 10 A for the PV inverter current, whereas the grid voltage, without the PV generator, V_0 = 230V: it can be argued that the Thévenin impedance is around 0.7Ω.

As an example of the Load Standard method, Fig. 8 shows the waveforms $v_0(t)$, v(t) and i(t) obtained in the PV system # 3 by using a resistor as load standard. The *voltage drop* is around 12V. The value of impedance is consistent with the value of the PV inverter method.

Experimental tests have been carried out on the three phase network of the various systems. Table I reports a sample of these ones, in which the values of impedance are always lower than 1Ω.

VI. Conclusions

Two measuring methods (one active and the other passive) have been presented, both based on perturbations of the grid voltage, in order to evaluate the network impedance at the PCC of photovoltaic systems. The experimental values are greater than the values calculated on the basis of simplifying assumptions (zero-current for the loads connected into the grid).

Therefore, by these values of network impedance it is possible to assess the *maximum current* and *power capacity* of the PV systems, which can be connected to the PCC in order to satisfy the Distributor upper limit of grid voltage (usually 110% of the nominal system voltage).

Generally, in the PV systems under study the PV power could be upgraded (double or more) without the need of particular change in the grid structure (increase of cable sections).

Finally, it should be stressed that an installation of high PV power (e.g. 20% of the transformer nominal power), which must be balanced in the three phases, could require a change of the turns ratio of the MV-LV transformer ("no-load tap changer") so as to reduce the e.m.f. of LV winding.

The results presented have taken into account the voltage waveforms at fundamental frequency. Further work is in progress to test different types of load standards, in order to obtain a suitable characterisation of the voltage drop, taking into account the waveform distortion. In this case, using a load standard with pronounced capacitive component should result in strong perturbations in the voltage waveforms and provide better effects, at the aim of assessing the network impedance at higher harmonic orders.

Acknowledgment

The authors wish to thank very much Dr.s P. Stirano, A. De Bonis and C. Di Steffano for the constant application during the measurements. Furthermore, many thanks to AMIAT S.p.A., "Provincia di Cuneo" and "Environment Park" for the constant support.

References

[1] Y. Ueda, T. Oozeki, K. Kurokawa et Al., "Analytical Results of Output Restriction due to the Voltage Increasing of Power Distribution Line in Grid-connected Clustered PV Systems", 31th IEEE PV Specialists Conference, Proc. pp. 1631-1634, Orlando, Florida, Jan., 2005.

[2] A. de Oliveira, J. C. de Oliveira, J. W. Resende and M. S. Miskulin, "Practical approaches for AC System Harmonic Impedance Measurements", IEEE Transactions on Power Delivery, Vol. 6 No. 4, pp 1721-1726, Oct. 1991.

[3] D. Schulz and R. Hanitsch, "Islanding detection in Germany: current standards and development",17th European PV Solar Energy Conference, Proc. pp.520-523, Munich, Germany, Oct. 2001.

[4] W. Xu, E. E. Ahmed, X. Zhang and X. Liu, "Measurement of Network Harmonic Impedances: Practical Implementation Issues and Their Solutions", IEEE Transactions on Power Delivery, Vol. 17 No. 1, pp 210-216, Jan. 2002.

[5] L. Asiminoaei, R. Teodorescu, F. Blaabjerg and U. Borup, "A New Method of On-line Grid Impedance Estimation for PV Inverter", 19th IEEE APEC '04, Applied Power Electronics Conference, Vol. 3, pp 1527-1533, 2004.

[6] S. Favuzza, G. Graditi, F. Spertino and G. Vitale, "Comparison of Power Quality of Different Photovoltaic Inverters: the viewpoint of the grid", International Conference on Industrial Technology IEEE ICIT, Proc. in CD Rom, pp 1-6, Hammamet, Tunisia, Dec. 2004.

[7] International Electrotechnical Commission, "Photovoltaic systems: characteristics of the utility interface", IEC Standard 1727, 1995.

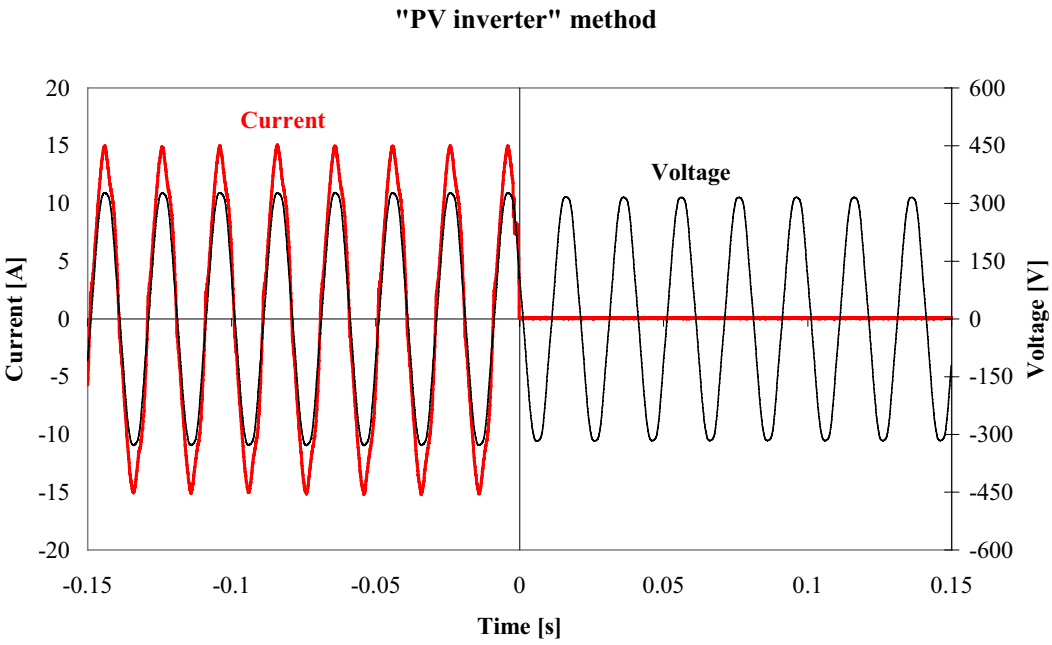

Fig. 7. Experimental results for grid-impedance evaluation according to the "PV inverter" method (system # 3).

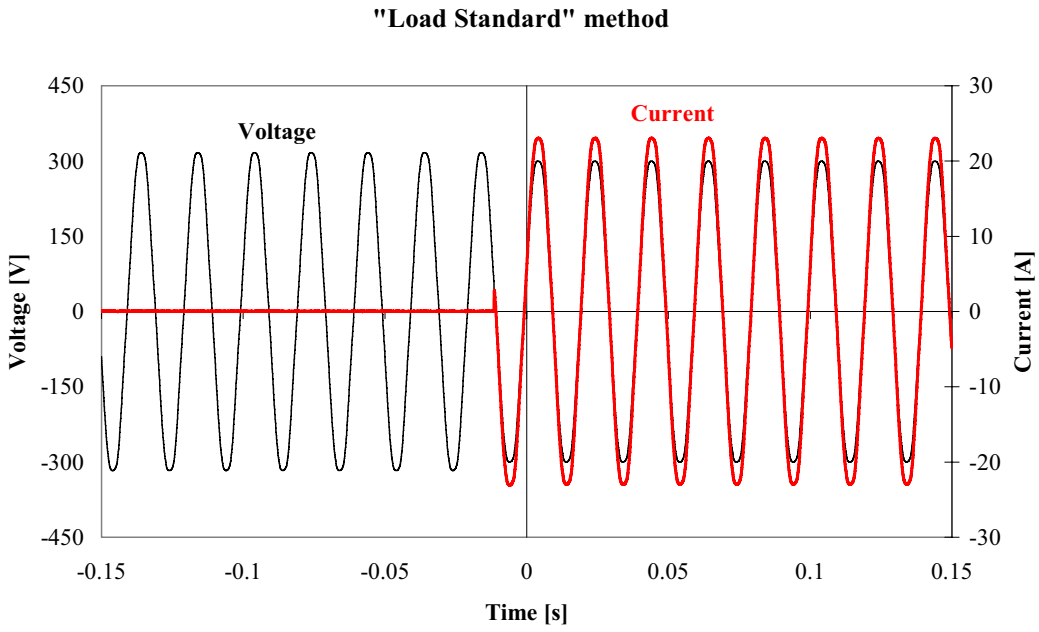

Fig. 8. Experimental results for grid-impedance evaluation according to the "Load Standard" method (system # 3).

TABLE I
GRID IMPEDANCE VALUES FOR THREE PV SYSTEMS

	"PV inverter" method						"Load standard" method					
	Phase 1		Phase 2		Phase 3		Phase 1		Phase 2		Phase 3	
System #	R [mΩ]	X [mΩ]	R [mΩ]	X [mΩ]	R [mΩ]	X [mΩ]	R [mΩ]	X [mΩ]	R [mΩ]	X [mΩ]	R [mΩ]	X [mΩ]
1	310	650	320	450	370	230	360	540	340	580	360	360
2	360	390	350	150	360	530	320	390	310	580	310	510
3	760	480	730	650	690	180	720	370	720	740	760	140